Eur. Phys. J. A **5**, 105–110 (1999)

THE EUROPEAN PHYSICAL JOURNAL A

The reaction $pp \to p\Lambda K^+$ near threshold

N. Kaiser

Physik Department T39, Technische Universität München, D-85747 Garching, Germany

Received: 28 October 1998 / Revised version: 12 January 1999
Communicated by F. Lenz

Abstract. We analyze the recent total cross section data for $pp \to p\Lambda K^+$ near threshold measured at COSY. Using an effective range approximation for the on-shell $p\Lambda$ S-wave final state interaction we extract from these data the combination $\mathcal{K} = \sqrt{2|K_s|^2 + |K_t|^2} = 0.38$ fm^4 of the singlet (K_s) and triplet (K_t) threshold transition amplitudes. We present an exploratory calculation of various (tree-level) vector and pseudoscalar meson exchange diagrams. Pointlike ω-exchange alone and the combined (ρ^0, ω, K^{*+})-exchange can explain the experimental value of $\mathcal{K}$. The pseudoscalar meson exchanges based on a SU(3) chiral Lagrangian turn out to be too large. However, when adding π^0-exchange in combination with the resonant $\pi N \to S_{11}(1650) \to K\Lambda$ transition and introducing monopole form factors with a cut-off $\Lambda_c = 1.5$ GeV one is again able to reproduce the experimental value of $\mathcal{K}$. More exclusive measurements are necessary to reveal the details of the $pp \to p\Lambda K^+$ production mechanism.

PACS. 13.60.Le Meson production – 13.75.Ev Hyperon-nucleon interactions

1 Introduction and summary

With the advent of the proton cooler synchrotron COSY at Jülich high precision data for associated strangeness production in proton-proton collisions, $pp \to p\Lambda K^+$, have become available in the near threshold region [1–3]. These data are of interest in several respects. First, they can provide a possibility to test various theoretical models of the strangeness dissociation mechanism for the nucleon. Secondly, the cross sections for strangeness production in the elementary pp-collision are an important input into transport model calculations of the strangeness production in heavy ion collisions. The latter may provide information about the hot and dense state of nuclear matter or the formation of the quark-gluon plasma. Various dynamical models have been developed for the reaction $pp \to p\Lambda K^+$ in [4,5] which in particular focus on the role of the $S_{11}(1650)$ nucleon resonance decaying into $K\Lambda$.

In a recent work [6] we have developed a novel approach to pion and eta production in proton-proton collisions, $pp \to pp\pi^0, pn\pi^+, pp\eta$, near threshold. In this approach one starts from the invariant T-matrix at threshold in the center-of-mass frame which is parametrized in terms of one (or two) constant threshold amplitudes. Close to threshold the relative momentum of the nucleons in the final state is very small and their empirically known strong S-wave interaction plays an essential role in the description of the meson-production data. In fact is was found in [6] that in all three cases the energy dependence of the total cross section near threshold is completely and accurately determined by the three-body phase space and the on-shell S-wave NN final state interaction (in the case $pp \to pp\eta$ also the S-wave ηN-interaction was included). Close to threshold the final state interaction can even be treated in effective range approximation using the well-known values of the scattering lengths and effective range parameters. Note that [6] gives a (partial) derivation of such an approach to final state interaction in the context of effective field theory (i.e. using only Feynman diagrams). Once one accepts such a phenomenological separation of the (on-shell) final state interaction from the full production process, one can extract from the total cross section data an experimental value of the constant threshold amplitude parametrizing the T-matrix. In the next step a standard Feynman diagram calculation is performed for the center-of-mass T-matrix at threshold. It was stressed in [6] that the evaluation of the Feynman diagrams has to be done fully relativistically since non-relativistic approximations will in general fail to reproduce correctly certain nucleon propagators. The source of this problem is the extreme kinematics of the meson-production process with the external center-of-mass momentum $|\boldsymbol{p}\,| \simeq \sqrt{M m_{\pi,\eta}}$ being proportional to the square root of the nucleon and meson mass. As a major result it was found in [6] that already the well-known tree-level (pseudoscalar and vector) meson exchange diagrams lead to predictions for the constant threshold amplitudes which agree with the corresponding experimental values within a few percent. It also turned out that the short range (ρ and ω) vector meson exchange dominates over the long range (π and η) pseudoscalar meson exchange for the processes $pp \to pp\pi^0, pn\pi^+, pp\eta$ at threshold.

The purpose of this work is to present a similar analysis for the kaon production channel $pp \to p\Lambda K^+$. After defining the threshold T-matrix for $pp \to p\Lambda K^+$ in terms of a singlet (K_s) and a triplet (K_t) transition amplitude and implementing the $p\Lambda$ S-wave final state interaction in effective range approximation, we extract from the COSY data an experimental value for the combination $\mathcal{K} = \sqrt{2|K_s|^2 + |K_t|^2} = 0.38$ fm^4. Next we perform a relativistic Feynman diagram calculation of various vector meson (ρ^0, ω, K^{*+}) and pseudoscalar meson (π^0, η, K^+) exchange diagrams with vertices given by a SU(3) symmetric (chiral) meson-baryon Lagrangian. We first evaluate these tree diagrams straightforwardly from the relativistic SU(3) Lagrangian not introducing ad hoc meson-nucleon form factors. The latter are a model-dependent and unobservable concept to account in some sense for the finite size of the hadrons involved. It is found that pointlike ω-exchange alone with coupling constants given by SU(3) symmetry can well reproduce the experimental value of $\mathcal{K} = 0.38$ fm^4. The total (ρ^0, ω, K^{*+}) vector meson exchange leads to $\mathcal{K} = 0.45$ fm^4 which is about 20% too large. Taking into account that possible SU(3) breaking effects and the uncertainty of the vector meson baryon coupling constant are of similar size, one can argue that the (pointlike) total vector meson exchange is still capable to explain the experimental value $\mathcal{K} = 0.38$ fm^4. The pseudoscalar meson (π^0, η, K^+) exchange diagrams with vertices given by the next-to-leading order SU(3) chiral Lagrangian give rise to rather large individual contributions. There is a tendency for cancelation between different types of diagrams, but with the SU(3) chiral meson-baryon vertices the effect is not pronounced enough. Interestingly, the (pointlike) K^+-exchange alone leads to $\mathcal{K} = 0.41$ fm^4 and if one omits the π^0-exchange one obtains $\mathcal{K} = 0.43$ fm^4 from the remaining $(\rho^0, \omega, K^{*+}, K^+, \eta)$-exchange diagrams. It therefore seems that the transition amplitude for $\pi N \to K\Lambda$ as given by the SU(3) chiral Lagrangian is not realistic. This is also underlined by the work of [7] in which these chiral amplitudes have been iterated to infinite orders via a coupled channel Lippmann-Schwinger equation and this way a good simultaneous fit of all available low energy data for pion (and photon) induced (η, K)-production could be found. We follow here [4,5] and add a π^0-exchange diagram involving the resonant $\pi N \to S_{11}(1650) \to K\Lambda$ transition. We assume the transition strength to be such that this process alone reproduces the near threshold data for $pp \to p\Lambda K^+$. If we furthermore introduce at each meson-baryon vertex a monopole form factor with a cutoff $\Lambda_c = 1.5$ GeV we finally end up with a total sum of the $S_{11}(1650)$-excitation graph and the vector and pseudoscalar meson exchange diagrams which again is in good agreement with the experimental value $\mathcal{K} = 0.38$ fm^4.

It becomes also clear from our analysis that the unpolarized total cross section data for $pp \to p\Lambda K^+$ do not provide enough information to distinguish different production mechanisms. In essence the information given by the total cross section data near threshold can be condensed into a single number, namely $\mathcal{K} = \sqrt{2|K_s|^2 + |K_t|^2} = 0.38$ fm^4. As we have demonstrated here, one can find various subprocesses (as e.g. the vector meson exchange, the K^+-exchange or the $S_{11}(1650)$-excitation focussed on in [4]) which alone can reproduce this value. More exclusive measurements of angular distributions and polarization observables for which one does not average out the kinematical complexity of the process $pp \to p\Lambda K^+$ due to spin and the three-particle final state are needed. Such measurements have been started [3] and we expect more data to come from COSY in the near future.

2 Threshold T-matrix

The T-matrix for kaon and lambda-hyperon production in proton-proton collisions, $p_1(\boldsymbol{p}\,) + p_2(-\boldsymbol{p}\,) \to p + \Lambda + K^+$, at threshold in the center-of-mass frame reads,

$$T_{\rm th}^{\rm cm}(pp \to p\Lambda K^+) = \frac{K_s}{\sqrt{3}}(i\boldsymbol{\sigma}_1 - i\boldsymbol{\sigma}_2 + \boldsymbol{\sigma}_1 \times \boldsymbol{\sigma}_2)\cdot \boldsymbol{p} + \frac{K_t}{\sqrt{3}} i(\boldsymbol{\sigma}_1 + \boldsymbol{\sigma}_2)\cdot \boldsymbol{p}, \quad (1)$$

where $\boldsymbol{p}$ is the proton center-of-mass momentum with $|\boldsymbol{p}\,| = 861.5$ MeV at threshold. The spin-operator $\boldsymbol{\sigma}_1$ is understood to be sandwiched between the spin-states of the ingoing proton $p_1(\boldsymbol{p}\,)$ and the outgoing proton, while $\boldsymbol{\sigma}_2$ acts between the proton $p_2(-\boldsymbol{p}\,)$ and the outgoing lambda. The (complex) amplitude K_s belongs to the singlet transition ${}^3P_0 \to {}^1S_0 s$ and the amplitude K_t belongs to the triplet transition ${}^3P_1 \to {}^3S_1 s$. The factor $1/\sqrt{3}$ was taken out for convenience since it appears naturally in a calculation employing SU(3) symmetry. We follow now the successful approach to pion and eta production of [6] and assume the T-matrix to be constant in the near threshold region and the energy dependence of the total cross section to be given by the three-body phase space and the (on-shell) $p\Lambda$ S-wave final state interaction. Since the outgoing proton and lambda have small relative momentum one treat their S-wave interaction in effective range approximation, i.e. in terms of the singlet and triplet $p\Lambda$ scattering lengths and the singlet and triplet $p\Lambda$ effective range parameters. Experimental evidence [8] and model calculations [9] suggest that these are rather similar for the ${}^1S_0$ and ${}^3S_1$ $p\Lambda$-states. In this case the unpolarized total cross section for $pp \to p\Lambda K^+$ including the $p\Lambda$ S-wave final state interaction reads,

$$\sigma_{\rm tot}(\epsilon) = (2|K_s|^2 + |K_t|^2)\frac{M^3 M_\Lambda \sqrt{s - 4M^2}}{48\pi^3 s^{3/2}} \times \int_{M+M_\Lambda}^{\sqrt{s}-m_K} \frac{dW}{W}\sqrt{\lambda(W^2, M^2, M_\Lambda^2)\lambda(W^2, m_K^2, s)} \times \bar{F}_{p\Lambda}(W), \quad (2)$$

with $\epsilon = \sqrt{s} - M - M_\Lambda - m_K$ the center-of-mass excess energy. M, M_Λ and m_K denote the proton, lambda and (charged) kaon mass. W is the $p\Lambda$ invariant mass with values between $M + M_\Lambda$ and the kinematical endpoint $\sqrt{s} - m_K$, and $\lambda(x, y, z) = x^2 + y^2 + z^2 - 2yz - 2xz - 2xy$

Table 1. Total cross sections for $pp \to p\Lambda K^+$. The data are taken from [2] and the fit is described in the text

ϵ [MeV]	0.68	1.68	2.68	3.68	4.68	5.68	6.68
$\sigma_{\rm tot}^{\rm exp}$ [nb]	2.1 ± 0.2	13.4 ± 0.7	36.6 ± 2.6	63.0 ± 3.1	92.2 ± 6.5	$135. \pm 11.$	$164. \pm 10.$
$\sigma_{\rm tot}^{\rm fit}$ [nb]	2.5	14.2	34.0	60.5	92.7	130.	171.

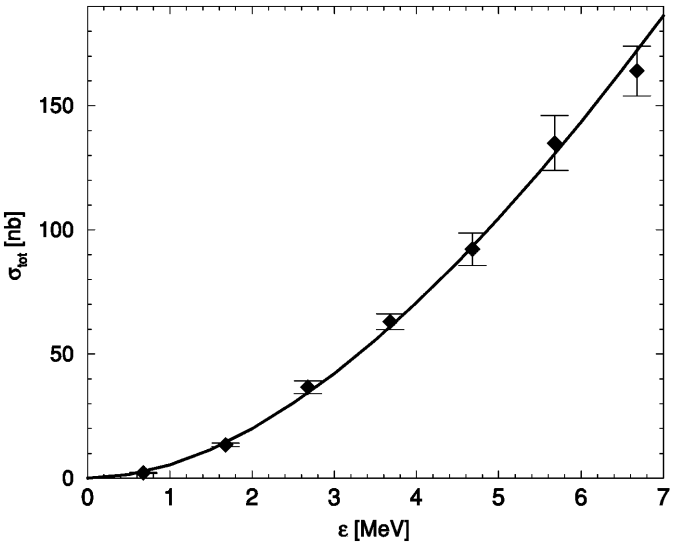

Fig. 1. Total cross sections for $pp \to p\Lambda K^+$ as a function of the center-of-mass excess energy $\epsilon = \sqrt{s} - M - M_\Lambda - m_K$. The data are taken from [2] and the full line is calculated with $\mathcal{K} = 0.38$ fm^4 and $p\Lambda$ final state interaction

denotes the Källen or triangle function. The correction factor from the (equal singlet and triplet) $p\Lambda$ S-wave final state interaction reads in effective range approximation,

$$\bar{F}_{p\Lambda}(W) = \left[1 + \frac{\bar{a}(\bar{a}+\bar{r})}{4W^2}\lambda(W^2, M^2, M_\Lambda^2) + \frac{\bar{a}^2\bar{r}^2}{64W^4}\lambda^2(W^2, M^2, M_\Lambda^2)\right]^{-1}. \quad (3)$$

We use for the $p\Lambda$ scattering length and effective range parameter the values $\bar{a} = 2.0$ fm and $\bar{r} = 1.0$ fm as extracted in [10] from the Dalitz plot distributions of the $pp \to p\Lambda K^+$ data and the low energy elastic $p\Lambda$ scattering cross sections. Using (2,3) for the total cross section, a best fit of the seven COSY data points near threshold [2] leads to the following experimental value of the combination

$$\mathcal{K} = \sqrt{2|K_s|^2 + |K_t|^2} = 0.38\,\text{fm}^4\,. \quad (4)$$

The resulting fit values of $\sigma_{\rm tot}$ are given in Table 1 and the energy dependent total cross section is shown in Fig. 1 for excess energies $\epsilon \leq 7$ MeV. Note that the best fit values at the two lowest energies $\epsilon = 0.68$ MeV and $\epsilon = 1.68$ MeV lie somewhat outside the experimental error band. This may be due to the neglect of the pK^+ Coulomb interaction. A similar slight overestimation of the data points closest to threshold was also observed in [6] for the reaction $pp \to pp\pi^0$. Compared to the processes $pp \to pp\pi^0, pn\pi^+, pp\eta$ studied in [6] the $p\Lambda$ final state interaction plays here a much less important role. This is also visible from Fig. 1 which shows that the data follow already approximately the pure three-body phase space behavior, i.e. $\sigma_{\rm tot}(\epsilon) \sim \epsilon^2$. Recently, three additional data points near threshold have been measured at COSY [11]: $\sigma_{\rm tot}(\epsilon = 8.6\,\text{MeV}) = (344 \pm 41)\,\text{nb}$, $\sigma_{\rm tot}(\epsilon = 10.9\,\text{MeV}) = (385 \pm 27)\,\text{nb}$ and $\sigma_{\rm tot}(\epsilon = 13.2\,\text{MeV}) = (505 \pm 33)\,\text{nb}$. These values are well reproduced by the present fit which predicts: 261 nb, 383 nb and 518 nb, respectively. We note aside that the two data points at higher excess energies $\sigma_{\rm tot}(\epsilon = 55\,\text{MeV}) = (2.7 \pm 0.3)\,\mu\text{b}$ and $\sigma_{\rm tot}(\epsilon = 138\,\text{MeV}) = (12.0 \pm 0.4)\,\mu\text{b}$ [3] come out according to (2) as $3.9\,\mu$b and $11.5\,\mu$b. The good agreement for $\epsilon = 138$ MeV should be regarded as accidental, since the same experiment [3] has measured a negative Λ recoil polarization, which can only result from S- and P-wave interference terms.

3 Diagrammatic approach

In this section we will present an exploratory calculation of various vector and pseudoscalar meson exchange diagrams contributing to the threshold amplitudes $K_{s,t}$ defined in (1). The coupling of vector mesons to baryons is described by the SU(3) symmetric Lagrangian,

$$\mathcal{L}_{VB} = \frac{g_V}{2}\left\{\text{tr}(\bar{B}\gamma_\mu[V^\mu, B]) + \text{tr}(\bar{B}\gamma_\mu B)\text{tr}(V^\mu)\right\}. \quad (5)$$

The SU(3)-matrices B and V^μ collect the octet baryon fields $(N, \Lambda, \Sigma, \Xi)$ and the octet vector meson fields $(\rho, \omega, K^*, \phi)$, respectively. The form (5) implies the relations $g_{\rho N} = g_V/2 = g_{\omega N}/3$ and $g_{\phi N} = 0$, and we use $g_V \simeq 6$ for the vector meson coupling constant. The pseudoscalar meson-baryon interaction is given by the chiral Lagrangians,

$$\mathcal{L}_{\phi B}^{(1)} = \frac{i}{8f_\pi^2}\text{tr}(\bar{B}\gamma_\mu[[\phi, \partial^\mu\phi], B]) + \frac{D}{2f_\pi}\text{tr}(\bar{B}\gamma_5\gamma_\mu\{\partial^\mu\phi, B\}) + \frac{F}{2f_\pi}\text{tr}(\bar{B}\gamma_5\gamma_\mu[\partial^\mu\phi, B]), \quad (6)$$

$$\mathcal{L}_{\phi B}^{(2)} = b_D\text{tr}(\bar{B}\{\chi_+, B\}) + b_F\text{tr}(\bar{B}[\chi_+, B]) + b_0\text{tr}(\bar{B}B)\text{tr}(\chi_+),$$
$$\chi_+ = 2\chi_0 - \frac{1}{4f_\pi^2}\{\phi, \{\phi, \chi_0\}\}, \quad (7)$$

with the diagonal matrix $\chi_0 = \text{diag}(m_\pi^2, m_\pi^2, 2m_K^2 - m_\pi^2)$. The SU(3)-matrix ϕ collects the octet pseudoscalar meson fields (π, K, η) and $f_\pi = 92.4$ MeV is the weak pion

Fig. 2. Vector meson exchange diagrams contributing to $pp \to p\Lambda K^+$

decay constant. $D \simeq 0.75$ and $F \simeq 0.50$ are the axial vector coupling constants as determined from semileptonic hyperon decays. The here most relevant $N\Lambda K$ coupling constant is given according to (6) as $g_{N\Lambda K} = -(D+3F)(M+M_\Lambda)/(2\sqrt{3}f_\pi) = -14.4$, which is rather close to the empirical value $g_{N\Lambda K} = -13.2$ of [12]. For the second order chiral Lagrangian $\mathcal{L}^{(2)}_{\phi B}$ only the explicit chiral symmetry breaking terms (linear in the quark masses) are displayed in (7). The coefficients $b_{D,F,0}$ are related to mass splittings in the baryon octet, the πN σ-term $\sigma_N(0) = (45 \pm 8)$ MeV and the (scalar) strangeness content of the nucleon. We use the values $b_D = 0.066$ GeV^{-1}, $b_F = -0.213$ GeV^{-1} and $b_0 = -0.304$ GeV^{-1}, found in [7]. At second order there exists in addition a large set of double-derivative terms ($\sim \partial_\mu\phi\partial_\nu\phi$) with a priori unknown coefficients. For the process $NN \to NN\pi$ it was observed in [6] that the explicit chiral symmetry breaking term is dominant at second order and therefore we neglect here the double-derivative terms with unknown coefficients.

3.1 Vector meson exchange

The vector meson exchange diagrams contributing to $pp \to p\Lambda K^+$ are shown in Fig. 2. Note that according to (5) both the $\Lambda\Lambda\rho^0$ and $\Lambda\Sigma^0\rho^0$ coupling vanish and therefore no ρ^0 exchange occurs in the right hand diagram where the K^+-meson is emitted from the proton line before the vector meson exchange.

Straightforward evaluation at threshold of the diagrams shown in Fig. 2 gives for ω-exchange,

$$\begin{aligned} K_t^{(\omega)} &= \frac{3g_V^2(D+3F)m_K(4M-m')}{8Mf_\pi(m_\omega^2+Mm')(2M+m')m'} \\ &= 0.38 \text{ fm}^4, \\ K_s^{(\omega)} &= \frac{3g_V^2(D+3F)m_K(m'-M)}{4Mf_\pi(m_\omega^2+Mm')(2M+m')m'} \\ &= -0.07 \text{ fm}^4, \end{aligned} \tag{8}$$

and for ρ^0-exchange,

$$\begin{aligned} K_t^{(\rho)} &= \frac{g_V^2(D+3F)m_K(2+\kappa_\rho)}{16Mf_\pi(m_\rho^2+Mm')(2M+m')}\left[\frac{m'}{4M}\kappa_\rho - 1\right] \\ &= 0.01 \text{ fm}^4, \\ K_s^{(\rho)} &= \frac{g_V^2(D+3F)m_K}{16Mf_\pi(m_\rho^2+Mm')(2M+m')} \\ &\quad \times \left[2 + \frac{3}{2}\kappa_\rho - \frac{m'}{8M}\kappa_\rho(6+5\kappa_\rho)\right] \\ &= -0.12 \text{ fm}^4. \end{aligned} \tag{9}$$

Note that we have included the large anomalous tensor-to-vector coupling ratio $\kappa_\rho \simeq 6$ in the $pp\rho^0$-vertex. For the $pp\omega$-vertex the tensor coupling is known to be small $\kappa_\omega \simeq 0$. The abbreviation m' stands for $m' = M_\Lambda - M + m_K = 671.0$ MeV. Furthermore, one finds from K^{*+}-exchange,

$$\begin{aligned} K_t^{(K^*)} &= 2K_s^{(K^*)} = -\frac{3g_V^2 F m_K}{2Mf_\pi(m_{K^*}^2+Mm')m'} \\ &= -0.24 \text{ fm}^4. \end{aligned} \tag{10}$$

For the K^{*+}-exchange diagram the intermediate state baryon can be either a Λ or a Σ^0 and we neglected the small mass difference $M_{\Sigma^0} - M_\Lambda = 77$ MeV in (10). In the absence of any empirical evidence, we did not include an anomalous tensor coupling in the $p\Lambda K^{*+}$-vertex. One observes that ω-meson exchange alone, (8), with $\mathcal{K}^{(\omega)} = 0.39$ fm^4, well reproduces the empirical value $\mathcal{K} = 0.38$ fm^4 extracted from the COSY data. Summing up all vector meson (ω, ρ^0, K^{*+})-exchange contributions one gets $\mathcal{K}^{(V)} = 0.45$ fm^4 which is about 20% too large. Taking into account, that the uncertainty of g_V and possible SU(3) breaking effects are of similar size one can still argue that (pointlike) vector meson exchange is able to explain the experimental value $\mathcal{K} = 0.38$ fm^4.

3.2 Pseudoscalar meson exchange

The pseudoscalar meson exchange diagrams contributing to $pp \to p\Lambda K^+$ are shown in Fig. 3. Two types of diagrams are possible, one where the meson rescatters via a chiral contact vertex, and another one with a baryon propagating in the intermediate state.

The calculation of the rescattering type diagrams in Fig. 3 gives for π^0-exchange,

$$\begin{aligned} K_t^{(\pi)} &= 2K_s^{(\pi)} \\ &= \frac{D+F}{16f_\pi^3(m_\pi^2+Mm')} \\ &\quad \times \Big[4(b_D+3b_F)(m_K^2+m_\pi^2) - 3(m'+m_K)\Big] \\ &= -0.95 \text{ fm}^4, \end{aligned} \tag{11}$$

for K^+-exchange,

$$\begin{aligned} K_t^{(K)} &= -2K_s^{(K)} \\ &= -\frac{D+3F}{4f_\pi^3(m_K^2+Mm')}\Big[8(b_0+b_D)m_K^2 + m' + m_K\Big] \\ &= -0.87 \text{ fm}^4, \end{aligned} \tag{12}$$

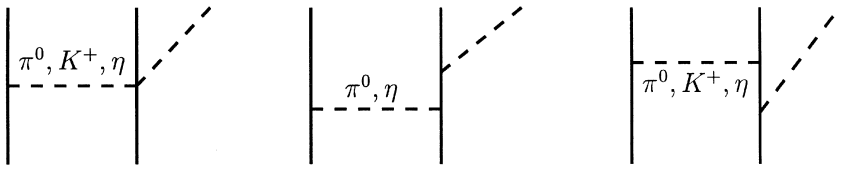

Fig. 3. Pseudoscalar meson exchange diagrams contributing to $pp \to p\Lambda K^+$

and for η-exchange,

$$K_t^{(\eta)} = 2K_s^{(\eta)} = \frac{D-3F}{48 f_\pi^3 (m_\eta^2 + Mm')} \times \Big[4(b_D+3b_F)(5m_K^2 - 3m_\pi^2) + 9(m'+m_K)\Big] = -0.25 \text{ fm}^4. \quad (13)$$

From the other diagrams in Fig. 3 with a baryon propagating in the intermediate state one finds for π^0-exchange,

$$K_t^{(\pi)} = 2K_s^{(\pi)} = \frac{(D+F)m_K}{8 f_\pi^3 (m_\pi^2 + Mm')(2M+m')} \times \Big[4D(D-F)M + (3D^2+2DF+3F^2)m'\Big] = 0.26 \text{ fm}^4, \quad (14)$$

for K^+-exchange,

$$K_t^{(K)} = -2K_s^{(K)} = \frac{(D+3F)(D^2+3F^2)m_K}{6 f_\pi^3 (m_K^2 + Mm')} = 0.54 \text{ fm}^4, \quad (15)$$

and for η-exchange,

$$K_t^{(\eta)} = 2K_s^{(\eta)} = \frac{(9F^2-D^2)m_K}{24 f_\pi^3 (m_\eta^2 + Mm')(2M+m')} \times \Big[D(4M+m') + 3Fm'\Big] = 0.12 \text{ fm}^4. \quad (16)$$

Numerically, the pseudoscalar meson exchange contributions generated by the SU(3) chiral Lagrangians (6,7) are too large, $K_t^{(ps)} = -1.16$ fm^4, $K_s^{(ps)} = -0.25$ fm^4. When combined with the vector meson exchange terms one would get $\mathcal{K}^{(V+ps)} = 1.28$ fm^4, which is about a factor 3 too large. Note that there is some tendency for cancelation between the rescattering type diagrams and the other ones, but the effect is not pronounced enough. It is interesting to observe that the pointlike K^+-exchange alone (12,15) gives $\mathcal{K}^{(K)} = 0.41$ fm^4 and if one omits the π^0-exchange (11,14) one obtains from the remaining contributions $\mathcal{K}^{(V+K+\eta)} = 0.43$ fm^4. Both these numbers are close to the experimental value $\mathcal{K} = 0.38$ fm^4. It therefore seems that the tree level $\pi N \to K\Lambda$ transition amplitude as given by the next-to-leading order chiral Lagrangian (5,6,7) has some unrealistic features. This is also underlined by the recent work of [7] in which these chiral amplitudes have been iterated to infinite order via a Lippmann-Schwinger equation and this way a good simultaneous fit of all available low energy data for pion (and photon) induced (η, K)-production could be found. Instead of performing a similar coupled channel calculation we follow here [4,5] and add a further π^0-exchange diagram involving the resonant $\pi N \to S_{11}(1650) \to K\Lambda$ transition. As argued in [4] we assume the corresponding transition strength to be so large that this process alone can reproduce the near threshold data for $pp \to p\Lambda K^+$. In this case one has the following contribution from $S_{11}(1650)$-excitation to the triplet and singlet threshold amplitudes,

$$K_t^{(N^*)} = 2K_s^{(N^*)} = 0.31 \,\text{fm}^4 \,. \quad (17)$$

We have convinced ourselves that the direct evaluation of the $S_{11}(1650)$-excitation graph leads to values of similar size taking into account the empirical ranges of the $S_{11}(1650)$-resonance mass and partial decay widths into πN and $K\Lambda$. Let us furthermore introduce a monopole form factor at each (off-shell) meson-baryon vertex with a cut-off $\Lambda_c = 1.5$ GeV. Such values of the cut-off Λ_c are typically used in one-boson exchange models [13] of the NN-interaction for both the pion- and vector-meson-nucleon vertex. This modification of the diagrams brings a reduction factor $(1 + Mm'/\Lambda_c^2)^{-2}$ for the vector and pseudoscalar meson exchange graphs. Note that in the case of the $S_{11}(1650)$-resonance contribution the form factor effect is already included in the number given in (17). Summing up all the contributions due to $S_{11}(1650)$)-excitation as well pseudoscalar and vector meson exchange (including the form factor) one finds $K_t^{(\text{tot})} = -0.31$ fm^4 and $K_s^{(\text{tot})} = -0.18$ fm^4. The resulting value $\mathcal{K}^{(\text{tot})} = 0.40$ fm^4 is again in good agreement with the empirical value $\mathcal{K} = 0.38$ fm^4.

Evidently, the main lesson to be learned from the present exploratory calculation is that there are in fact various subprocesses (like pointlike vector meson or K^+-exchange or the $S_{11}(1650)$-resonance excitation) which alone can explain the near threshold data for $pp \to p\Lambda K^+$. With reasonable assumptions on the various coupling strengths and the cut-off Λ_c entering the (unobservable) meson-nucleon form factor one finds that also the total sum of many processes is able to reproduce the near threshold data for $pp \to p\Lambda K^+$. This is possible because of

cancelations between terms of different sign and because of the freedom the to shift strength between the singlet (K_s) and triplet (K_t) threshold amplitude. Only more exclusive data (like angular distributions and polarization observables) can help to distinguish different $pp \to p\Lambda K^+$ production mechanisms.

Finally, we like to comment on the recently measured process $pp \to p\Sigma^0 K^+$. It was found experimentally [11] that the corresponding total cross sections near threshold are about a factor 30 smaller than those for $pp \to p\Lambda K^+$ (at equivalent excess energies). ω-meson exchange or K^+-exchange might offer an explanation for this suppression via the small SU(3)-ratio $g_{N\Sigma K}/g_{N\Lambda K} = -\sqrt{3}/9 \simeq -0.19$. An explicit calculation of the ω-exchange and K^+-exchange (using now $m' = M_{\Sigma^0} - M + m_K = 748$ MeV in (8,12,15)) gives for the $p\Sigma^0 K^+$-channel values of $\mathcal{K}^{(\omega)}_{\Sigma^0} = 0.06$ fm^4 and $\mathcal{K}^{(K)}_{\Sigma^0} = 0.09$ fm^4, i.e. a suppression factor of about 40 or 20 for the total cross section. However, such considerations may be too simplistic in the light of possible strong coupled channel effects [7] between $K\Lambda$- and $K\Sigma$-states.

References

1. J.T. Balewski et al., *Phys. Lett.* **B388** (1996) 859
2. J.T. Balewski et al., *Phys. Lett.* **B420** (1998) 211
3. R. Bilger et al., *Phys. Lett.* **B420** (1998) 217
4. G. Fäldt and C. Wilkin, *Z. Phys.* **A357** (1997) 241
5. A. Sibirtsev, *Phys. Lett.* **B359** (1995) 29; R. Shyam, nucl-th/9901038
6. V. Bernard, N. Kaiser and Ulf-G. Meißner, nucl-th/9806013, *Eur. Phys. J.* **A** (1999) 259
7. N. Kaiser, T. Waas and W. Weise, *Nucl. Phys.* **A612** (1997) 297
8. G. Alexander et al., *Phys. Rev.* **173** (1968) 1452; B. Sechi-Zorn et al., *Phys. Rev.* **175** (1968) 1735
9. M.M. Nagels et al., *Phys. Rev.* **D20** (1979) 1633; B. Holzenkamp et al., *Nucl. Phys.* **A500** (1989) 485; A. Reuber et al., *Nucl. Phys.* **A570** (1994) 543
10. J.T. Balewski et al., *Eur. Phys. J.* **A2** (1998) 99
11. S. Sewerin et al., nucl-ex/9811004
12. A.D. Martin, *Nucl. Phys.* **B179** (1981) 33
13. R. Machleidt, K. Holinde and Ch. Elster, *Phys. Reports* **149** (1987) 1